

Droplet Mobility on Lubricant-Impregnated Surfaces

J. David Smith^{1,†}, Rajeev Dhiman^{1,†}, Sushant Anand¹, Ernesto Garduno¹, Robert E. Cohen²,
Gareth H. McKinley¹ Kripa K. Varanasi^{1,*}

¹Department of Mechanical Engineering, Massachusetts Institute of Technology, Cambridge, MA 02139, USA.

²Department of Chemical Engineering, Massachusetts Institute of Technology, Cambridge, MA 02139, USA.

[†]equal contribution.

*Correspondence to: varanasi@mit.edu.

Supplementary Materials:

Materials and methods

Figures S1-S3

Tables S1-S3

Movies S1-S2

References (1-5)

Descriptive legends for each item of supplementary materials

Materials and methods

This section describes the method of fabricating the textured surfaces and procedure for conducting laser confocal fluorescence microscopy and contact angle measurements.

Figures S1 – S3

Figure S1 shows a SEM image of the silicon micropost array.

Figure S2 shows a SEM image of silicon microposts etched with nanograss.

Figure S3 shows SEM images of nanograss-covered silicon micropillars impregnated with an ionic liquid (BMIm).

Tables S1 – S3

Table S1: Goniometric contact angle measurements of the various liquids used in the study.

Table S2: Interfacial tension measurements of silicone oil in air and water environment.

Table S3: Relevant parameters of the textured substrates used in the study.

Videos S1 – S2

Video S1: This video shows the effect of lubricant viscosity on droplet velocity. Silicone oil of three different dynamic viscosities were chosen whereas the droplet liquid was water. The substrate was a silicon micropost array coated with octadecyltrichlorosilane (OTS) and inclined at 30 deg. to the horizontal.

Video S2: This video shows that the droplets in our experiments were rolling rather than sliding across the lubricant-impregnated substrate. The seed particles in the water droplet were ground coffee and the lubricant impregnated in the micropost array was silicone oil.

Materials and Methods

1. Lubricant-impregnated surfaces

The textured substrates used in this study were square microposts etched in silicon using standard photolithography process (Fig. S1). A photomask with square windows was used and the pattern was transferred to photoresist using UV light exposure. Next, reactive ion etching in inductively-coupled plasma was used to etch the exposed areas to form microposts. Each micropost had a square geometry with width $a = 10 \mu\text{m}$, height $h = 10 \mu\text{m}$, and varying edge-to-edge spacing $b = 5, 10, 25,$ and $50 \mu\text{m}$.

A second level of roughness was produced on microposts in some cases by creating nanograss (Fig. S2). For this purpose, Piranha-cleaned micropost surfaces were etched in alternating flow of SF_6 and O_2 gases for 10 minutes in inductively-coupled plasma.

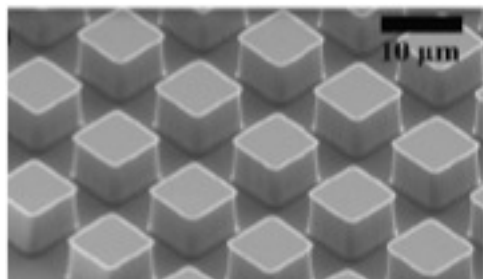


FIG. S1. SEM of silicon microposts

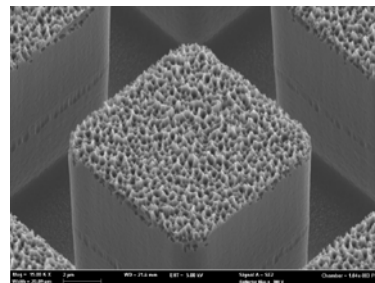


FIG. S2. SEM of silicon microposts with nanograss

The samples were then cleaned in a Piranha solution and treated with a low-energy silane (octadecyltrichlorosilane - OTS) by solution deposition. The samples were impregnated with lubricant by slowly dipping them into a reservoir of the lubricant. They were then withdrawn at speed S slow enough that capillary numbers $Ca = \mu_o S / \gamma_{oa} < 10^{-5}$ to ensure that no excess fluid remained on the micropost tops where μ_o is the dynamic viscosity and γ_{oa} is the surface tension of the lubricant. Note that when the advancing angle $\theta_{adv,os(a)}$ is less than θ_c (see Table S3) the lubricant film will not spontaneously spread into the textured surface, as can be seen for BMIm (1-butyl-3-methylimidazolium bis(trifluoromethylsulfonyl) imide) in Fig. S3. However, by withdrawing the textured surfaces from a reservoir of BMIm, the impregnating film remains stable, since $\theta_{rec,os(a)} < \theta_c$ for the microposts with $b = 5 \mu\text{m}$ and $10 \mu\text{m}$.

2. Laser confocal fluorescence microscope (LCFM) imaging

In order to determine whether or not the micropost tops were covered with lubricant after dipping, a LCFM (Olympus FV 300) was used. A fluorescent dye (DFSB-175, Risk Reactor, CA) was dissolved in the lubricant and the textured substrate was impregnated with the dyed lubricant using dip coating, as explained above. The dye gets excited at wavelengths of $\sim 400 \text{ nm}$ and the resulting emittance was captured by the microscope. As the focused laser beam scanned through the sample, areas containing dye appeared bright, indicating the presence of lubricant. This is

shown in Fig. 1g on substrates impregnated with silicone oil. In contrast, BMIm doesn't wet post tops, which therefore appear dark (Fig. 1h).

3. Contact angle measurements

Contact angles of silicone oil and BMIm were measured on the OTS-coated silicon surfaces in the presence of air and DI water using a Ramé-Hart Model 500 Advanced Goniometer/Tensiometer. The advancing ($\theta_{adv,os(a)}$, $\theta_{adv,os(w)}$) and receding ($\theta_{rec,os(a)}$, $\theta_{rec,os(w)}$) angles were taken as an average of at least 8 measurements. 5 μl droplets were deposited at a volume addition/subtraction rate of 0.2 $\mu\text{l s}^{-1}$, yielding contact line velocities V_c less than 1 mm min^{-1} . The resulting capillary numbers were $Ca = \mu_o V_c / \gamma_{o(i)} < 10^{-5}$ ensuring that the measured dynamic contact angles were essentially the same as contact angles obtained immediately after the contact line comes to rest.¹⁻⁴ The measured contact angles are reported in Table S1.

Table S1. Contact angle measurements on smooth OTS-treated silicon surfaces. It is important to note that a surface that has been dipped in silicone oil maintains an oil film on the surface after a water droplet is deposited because the film cannot dewet the surface since $\theta_{rec,os(w)} = 0^\circ$. Therefore, an oil-water-solid contact line cannot exist and pinning forces must be zero. Accordingly, the oil-solid-water pinning term in Eq.'s (10) and (11) should be neglected if $\theta_{rec,os(w)} = 0^\circ$. Similarly oil-solid-air pinning term should be neglected if $\theta_{rec,os(a)} = 0^\circ$. For this reason, pinning forces are taken to be zero in Fig. 3 for silicone oil, even though $\cos\theta_{rec,os(w)} - \cos\theta_{adv,os(w)} > 0$.

Liquid	Substrate	$\theta_{adv,os(a)}$ ($^\circ$)	$\theta_{rec,os(a)}$ ($^\circ$)	$\theta_{adv,os(w)}$ ($^\circ$)	$\theta_{rec,os(w)}$ ($^\circ$)
Silicone oil	OTS-treated silicon	0	0	20 ± 5	0
BMIm	OTS treated silicon	67.8 ± 0.3	60.8 ± 1.0	61.3 ± 3.6	12.5 ± 4.5
DI water	OTS-treated silicon	112.5 ± 0.6	95.8 ± 0.5	NA	NA
Silicone oil	Silicon	0	0	153.8 ± 1.0	122 ± 0.8
BMIm	Silicon	23.5 ± 1.8	9.8 ± 0.9	143.4 ± 1.8	133.1 ± 0.9
DI water	Silicon	$20 \pm 5^\circ$	0	NA	NA

Table S2. Surface and interfacial tension measurements and resulting spreading coefficients, $S_{ow(a)} = \gamma_{wa} - \gamma_{ow} - \gamma_{oa}$, of 9.34, 96.4, and 970 cP Dow Corning PMX 200 Silicone oils on water in air. Values of γ_{ow} were taken from Ref. 5, and values of γ_{oa} were provided by Dow Corning.

Liquid	γ_{ow} (mN/m)	γ_{oa} (mN/m)	γ_{wa} (mN/m)	$S_{ow(a)}$ (mN/m)
Silicone oil (9.34 cP, 96.4 cP)	46.7	20.1	72.2	5.4
Silicone oil (970 cP)	45.1	21.2	72.2	5.9

Table S3. Texture parameters b , r , ϕ , and critical contact angles θ_c defined by $\theta_c = \cos^{-1}((1-\phi)/(r-\phi))$; h , $a = 10 \mu\text{m}$ for all substrates tested. Note if the silicon substrate is not coated with OTS, $\theta_{os(w)} > \theta_c$ for both lubricants and all b . Thus water droplets should displace the lubricant and get impaled by the microposts leading to significant pinning, which was confirmed as such droplets did not roll-off of these surfaces.

Post spacing, b (μm)	r	ϕ	θ_c ($^\circ$)
5	2.8	0.44	76
7.5	2.3	0.33	70
10	2.0	0.25	65
25	1.3	0.08	42
50	1.1	.093	26

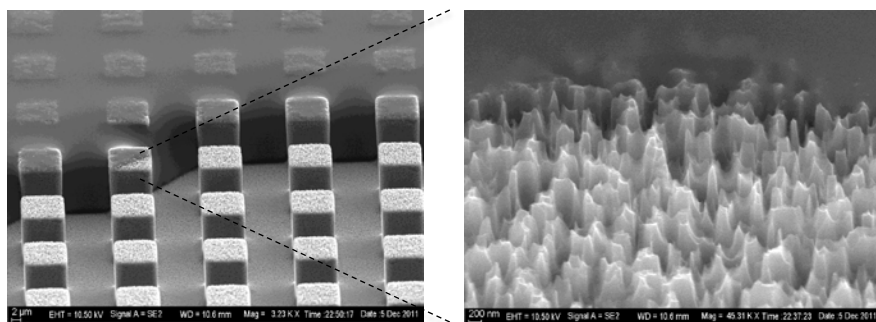


FIG. S3. SEM images of a pinned BMIm contact line. BMIm completely fills the voids between the nano-ridges (right), resulting in almost no exposure of the solid surface to air after dipcoating ($\phi \cong 0$).

References

1. M. Strobel and C. S. Lyons, *Plasma Processes and Polymers*, 2011, **8**, 8-13.
2. F. Garbassi, M. Morra and E. Occhiello, *Polymer surfaces from physics to technology*, Wiley, 1994.
3. Y. Uyama, H. Inoue, K. Ito, A. Kishida and Y. Ikada, *Journal of Colloid and Interface Science*, 1991, **141**, 275-279.
4. L. M. Lander, L. M. Siewierski, W. J. Brittain and E. A. Vogler, *Langmuir*, 1993, **9**, 2237-2239.
5. C.Y. Wang, R.V. Calabrese, *AIChE J.* 1986, **32**, 667.